International Journal of Pure and Applied Physics. ISSN 0973-1776 Volume 13, Number 1 (2017), pp. 79-83

On the impact parameter dependence of the peak mass production

Sukhjit Kaur*
SGGS College Sector-26 Chandigarh-160 019 INDIA
sukhjitkaur.pu@gmail.com

***Abstract*—We study the effect of colliding geometry on the peak center-of-mass energy ($E_{c.m.}^{max}$) and peak multiplicity of intermediate mass fragments ($<N_{IMF}>^{max}$) for symmetric neutron-rich colliding pairs. We find that with increase in the impact parameter, both $<N_{IMF}>^{max}$ and $E_{c.m.}^{max}$ show a rise and fall. In order to explain this behavior, we study the rapidity distribution of the intermediate mass fragments at their respective $E_{c.m.}^{max}$ and also at energies below and above $E_{c.m.}^{max}$ for the reaction of $^{40}Ca+^{40}Ca$. We also check the role of neutron content on $E_{c.m.}^{max}$ and $<N_{IMF}>^{max}$ for isotopic as well as isobaric colliding pairs.**

***Index Terms*—Peak center-of-mass energy; peak multiplicity of intermediate mass fragments; IQMD model; impact parameter**

I. INTRODUCTION

An excited nuclear system formed in energetic nucleus-nucleus collisions, depending on the excitation energy deposited in the system, decays via emission of fragments of various sizes such as free-nucleons, light charged particles (LCPs), intermediate mass fragments (IMFs) etc. It is now well known that bombarding energy and collision geometry of a reaction play an important role in deciding the fate of the reaction [1−6]. In nucleus-nucleus collisions, the density achieved in the overlapping region is well above the normal nuclear matter density. The nucleons which are located in the geometrical overlap of the projectile and target constitute the participant matter whereas nucleons from non-overlapping region constitute the spectator matter. The spectator matter has a little excitation energy and they continue with nearly the original velocity. In central heavy-ion collisions, most of the nucleons constitute the participant matter and excitation energy is very high that results in a fast explosion of nuclei into light fragments and a very few medium size fragments are formed. With an increase in the impact parameter, interaction volume goes on decreasing and spectator matter increases. As a result, the formation of light fragments diminishes and intermediate and heavy fragment formation dominates.

In the literature, several attempts have been made to study the role of collision geometry in multifragmentation [2,3,5−7], flow [8] and nuclear stopping [9]. Ogilvie *et al*. [5] studied the asymmetric nuclear collisions at a bombarding energy of 600 MeV/nucleon. They found that with increase in the violence of the collisions, average multiplicity of IMFs first increases to a maximum and then decreases again. Later on, Tsang *et al*. [6] investigated the impact of collision geometry on the fragment production for reaction of $^{197}Au+^{197}Au$ at E = 100, 250 and 400 MeV/nucleon. They found that at E = 100 MeV/nucleon, average number of IMFs decreases with the increase in the impact parameter, whereas for energies of 250 and 400 MeV/nucleon, a "rise and fall" in the production of IMFs is observed with change in impact parameter. Also with increase in the incident energy, the peak IMF multiplicity gets shifted to higher impact parameters. Also INDRA and ALADIN Collaborations [7] studied peripheral collisions of $^{197}Au+^{197}Au$ at incident energies between 40 and 150 MeV/nucleon using 4π multidetector. They observed that the maximum of fragment production is located near the mid rapidity region for lower incident energies that moves gradually towards projectile and target rapidities with increase in the incident energy. Puri and Kumar [3] carried out a systematic study of the fragment production in the reaction of $^{40}Ca+^{40}Ca$ at incident energies between 20 and 1000 MeV/nucleon and over full impact parameter range (i.e., from b = 0 to b_{max}). They found that IMF multiplicity attains a maximum at central collisions and it gradually decreases with increase in the impact parameter at lower incident energies whereas an explicit rise and fall is observed at energies above 150 MeV/nucleon. Vermani and Puri [2] also studied the rise and fall of IMFs for reaction of $^{197}Au+^{197}Au$ at E = 400, 600 and 1000 MeV/nucleon with change in colliding geometry. For a particular collision geometry, IMF multiplicity is found to increase with beam energy at low energies. As the energy increases, excess energy makes the IMFs to break up into smaller fragments [10]. The latter phenomenon dominates at higher incident energies and the production of IMFs should decrease due to the transition into the gas phase of nuclear matter [6]. Thus, the energy at which maximal production of IMFs occurs may be considered as the energy at which the phase transition occurs. For central colliding geometry, a "rise and fall" in the production of IMFs is observed with change in the incident energy. In Refs. [10,11], it is found that both the peak multiplicity of IMFs ($\langle N_{IMF}\rangle^{max}$) and energy at which the maximum number of IMFs are emitted ($E_{c.m.}^{max}$) scale with the composite system mass. But no study is made to check the role of collision geometry on $E_{c.m.}^{max}$ and $\langle N_{IMF}\rangle^{max}$.

All the above mentioned studies have been carried out for systems lying close to the line of stability. The availability of radioactive-ion beam (RIB) facilities [12] has opened up a new dimensions to study the collisions of neutron-rich nuclei.

The author is thankful to Professor Rajeev K. Puri, Department of Physics, Panjab University, Chandigarh-160014, for fruitful discussions on the present work.
*Department of Physics, SGGS College, Sector-26, Chandigarh-160019, INDIA. (email: sukhjitkaur.pu@gmail.com)

Recently, the production cross sections for new exotic isotopes ^{47}P, ^{51,53,55,57}Cl, ^{52,54}Ar, ^{56,58,60}Ca, ^{59,61,63}Sc, and ^{62,64,66}Ti are predicted to be larger than 0.1 pb [13]. Thus, there is a possibility for these nuclei to be synthesized and detected at present experimental possibilities. The predicted cross sections seem to be optimistic, especially for the isotopes of Ca, Sc, and Ti. In Ref. [14], the production cross sections for neutron-rich nuclei from fragmentation of ^{76}Ge beam has been studied. They observed neutron-rich nuclides of the elements with charge number in the range of 17 to 25 (^{50}Cl, ^{53}Ar, ^{55,56}K, ^{57,58}Ca, ^{59,60,61}Sc, ^{62,63}Ti, ^{65,66}V, ^{68}Cr, and ^{70}Mn). The neutron content of a colliding pair is found to affect the fragment production [15,16]. Recently, Puri and co-workers [17] studied the effect of isospin degree of freedom on $\langle N_{IMF}\rangle^{max}$ and $E_{c.m.}^{max}$. This study was limited for semi-central collisions only. It would be interesting to see the role colliding geometry on $E_{c.m.}^{max}$ and $\langle N_{IMF}\rangle^{max}$. Here we extend this study over entire colliding geometry from central to peripheral one and would like to analyze whether there is any difference in the outcome for peripheral collisions.

II. THE MODEL

The present study is carried out within the framework of isospin-dependent quantum molecular dynamics (IQMD) model [18] which treats different charge states of nucleons, Δ's, and pions explicitly. In addition to the use of explicit charge states of all baryons and mesons, a symmetry potential between protons and neutrons corresponding to the Bethe–Weizsäcker mass formula has been included. Isospin effects come into the picture due to the interplay between the Coulomb potential, isospin-dependent cross section, and symmetry potential. Two nucleons undergo a scattering if they are closer than a certain minimum distance. The cross section for neutron–neutron collisions is taken to be equal to the proton–proton cross section and cross section for neutron–proton is taken to be three times the neutron–neutron (proton–proton) cross section. This scattering is further subjected to the fulfillment of Pauli principle. In IQMD model, explicit Pauli blocking is included i.e., Pauli blockings of the neutrons and of the protons are treated separately. Any scattering that violates the Pauli principle is neglected. Whenever an attempted collision is blocked, the scattering partners maintain the original momenta prior to scattering. The phase space generated is analyzed using the minimum spanning tree (MST) method [19].

III. RESULTS AND DISCUSSION

We simulated several thousands of events for Ne+Ne, Al+Al, Cl+Cl, and Ca+Ca reactions at incident beam energies between 30 and 150 MeV/nucleon. In particular, we simulated the reactions of ^{34}Cl+^{34}Cl (N/Z = 1.0), ^{34}Al+^{34}Al (N/Z = 1.6), ^{34}Ne+^{34}Ne (N/Z = 2.4), ^{40}Ca+^{40}Ca (N/Z = 1.0) and ^{60}Ca+^{60}Ca (N/Z = 2.0) over the whole impact parameter range (from b/b_{max} = 0.0 to 0.8). Here, we have chosen symmetric colliding pairs because in symmetric collisions, even at low incident energies, system has enough excitation energy to undergo multifragmentation compared to asymmetric collisions. We, here, use a soft equation of state (EOS) along with standard isospin- and energy-dependent cross section and reactions are followed till 300 fm/c. The results with the above choice of EOS, cross section and clusterization algorithm were in good agreement with the experimental data [17]. This choice of soft EOS is also supported by several studies where kaon probe

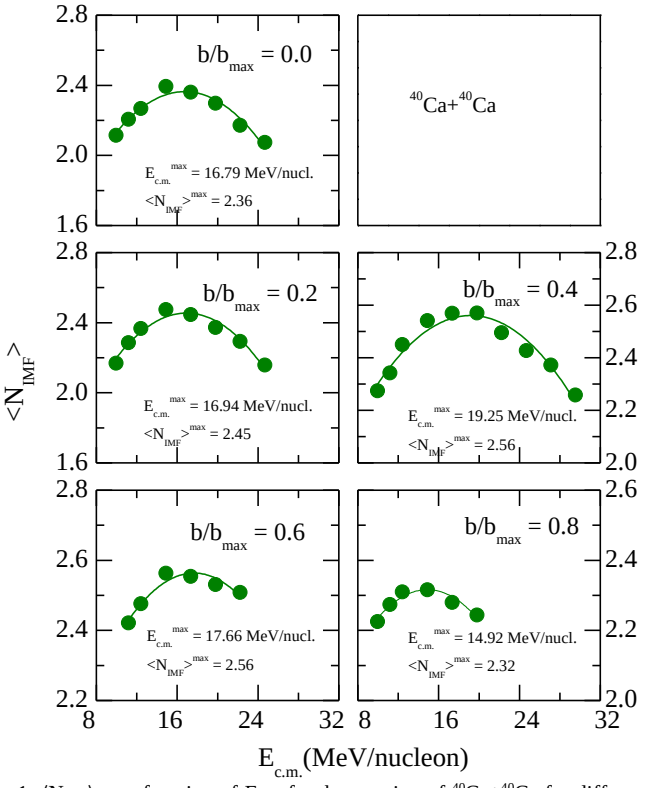

Fig. 1. $\langle N_{IMF}\rangle$ as a function of $E_{c.m.}$ for the reaction of ^{40}Ca+^{40}Ca for different colliding geometries. Solid curves show the quadratic fit to theoretical calculations to estimate the peak center-of-mass energy at which the maximal IMF emission occurs.

[20] and flow [8, 21] were used to pin down the soft nature of the matter.

In Fig. 1, we display the average multiplicity of intermediate mass fragments (IMFs, $5 \leq A \leq A_{tot}/6$, where A_{tot} is composite system mass) as a function of incident energy in the center-of-mass frame for the reaction of ^{40}Ca+^{40}Ca at different collision geometries. The solid circles represent our theoretical calculations and lines represent the quadratic fits to the theoretical points. It is clear from fig. that multiplicity of the IMFs shows a universal "rise and fall" of fragment production with an increase in the incident beam energy for all collision geometries. At low incident beam energies, the larger fraction of the initial energy is carried away by the pre-equilibrium nucleonic emission and the system does not have sufficient energy to break a colliding pair into a large number of IMFs and heavier fragments. Thus, very small number of IMFs are emitted. As beam energy is increased, system will have more and more energy to break colliding nuclei into a large number of IMFs. With further increase in the beam energy, even more compressional energy will be available that leads to break up of the nuclear system into free nucleons and lighter fragments. The number of IMFs first increases with increase in the incident energy, attains a maxima at a particular value of the incident energy ($E_{c.m.}^{max}$) and then decreases with further increase in the incident energy.

In Fig. 2, we display the impact parameter dependence of $\langle N_{IMF}\rangle^{max}$ (upper panel) and $E_{c.m.}^{max}$ (lower panel) for reactions of $^{40}Ca+^{40}Ca$ and $^{60}Ca+^{60}Ca$. $\langle N_{IMF}\rangle^{max}$ and corresponding $E_{c.m.}^{max}$ are obtained by making quadratic fit to the model calculations for $\langle N_{IMF}\rangle$ as a function of $E_{c.m.}$ (see Fig. 1). From

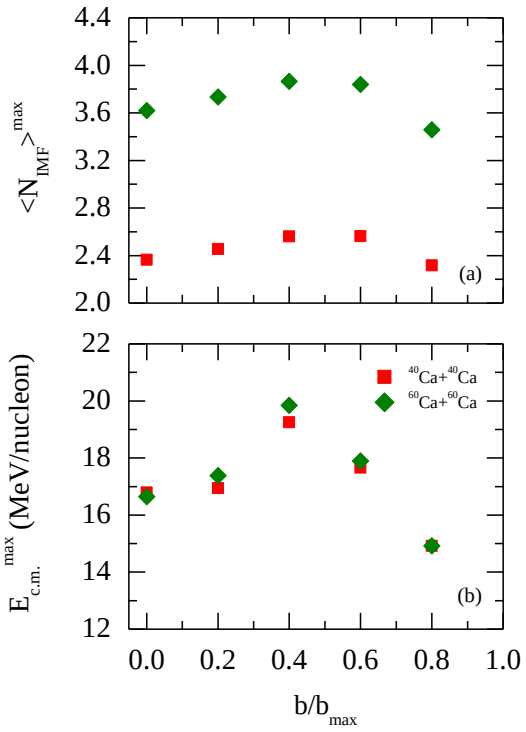

Fig. 2. (Color Online) $\langle N_{IMF}\rangle^{max}$ (upper panel) and $E_{c.m.}^{max}$ (lower panel) as a function of impact parameter.

Fig. 2(a), we find that $\langle N_{IMF}\rangle^{max}$ first increases with increase in the impact parameter, attains a maximum value and then decreases at peripheral geometries. In case of central geometries, the excitation energy is very high. The nuclear matter breaks into much smaller pieces and IMFs or heavy-mass fragments are formed rarely. In Ref. [4], it has been discussed that free-nucleons and LCPs are emitted from the mid-rapidity whereas IMFs and heavy fragments are the remnants of spectator matter. With increase in the impact parameter, the degree of spectator matter increases, as a result number of IMFs increases. With further increase in the impact parameter i.e., for peripheral geometries, system do not possess sufficient energy to excite the nuclear matter and therefore heavier residual fragments survive and few IMFs, LCPs or free-nucleons are formed. Thus, the maximum number of IMFs are seen only between semi-central and semi-peripheral impact parameters. Also $\langle N_{IMF}\rangle^{max}$ increases with the increase in system mass as we move from $^{40}Ca+^{40}Ca$ to $^{60}Ca+^{60}Ca$. Here, the range of IMFs for $^{40}Ca+^{40}Ca$ is from A = 5 to 13 whereas in case of $^{60}Ca+^{60}Ca$, it is from A = 5 to 20. The increase in $\langle N_{IMF}\rangle^{max}$ with increase in system mass could be due to difference in mass range of IMFs. To make this point clear, we checked $\langle N_{IMF}\rangle^{max}$ by taking same definition of IMFs for both systems and found that trend remains unaltered though difference in $\langle N_{IMF}\rangle^{max}$ for both systems decreases. This has also been supported by Ref. [11] where mass range for IMFs was considered to be same for all systems.

From Fig. 2(b), we see that $E_{c.m.}^{max}$ is same for the reactions of $^{40}Ca+^{40}Ca$ and $^{60}Ca+^{60}Ca$. In previous studies [17], it has been shown that $E_{c.m.}^{max}$ increases with increase in system mass but decreases with increase in isospin asymmetry. Here, both mass and neutron content increase. Both these variations cancel each other and no change is observed in $E_{c.m.}^{max}$. From

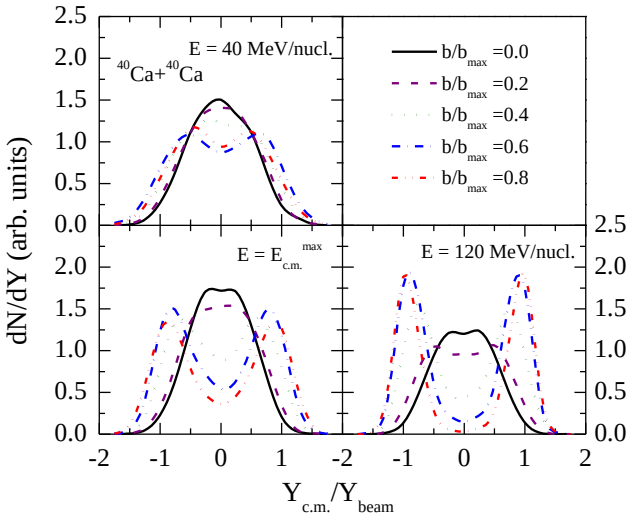

Fig. 3. (Color Online) The rapidity distribution, dN/dY, as a function of reduced rapidity, $Y_{c.m.}/Y_{beam}$ for the reaction of $^{40}Ca+^{40}Ca$ for all collision geometries at their respective $E_{c.m.}^{max}$ and at below and above $E_{c.m.}^{max}$.

Fig. 2(b), we find that $E_{c.m.}^{max}$ first increases with increase in the impact parameter, attains a maxima and then decreases at peripheral geometries. With increase in impact parameter, system will need more and more energy to form a sufficient number of IMFs. At peripheral geometries, IMFs mainly come from spectator region and are obtained at lower energies. With increase in incident energy, interaction time will decrease and hence momentum will not get transferred among nucleons and only heavy residual fragments will survive along with few lighter fragments and free-nucleons.

To shed light on the contribution of participant/spectator matter towards IMFs, in Fig. 3, we plot the rapidity distribution of IMFs for reaction of $^{40}Ca+^{40}Ca$ for all collision geometries at their respective $E_{c.m.}^{max}$ and also at below and above $E_{c.m.}^{max}$. Solid, dashed, dotted, dash-dotted, dash-double-dotted lines represent rapidity distribution of IMFs at b/b_{max} = 0.0, 0.2, 0.4, 0.6 and 0.8, respectively. From Fig. 3, we find that in case of central geometries, there is a single Gaussian. It implies that IMFs are mainly coming from mid rapidity region. As we move towards peripheral collisions, the Gaussian gets broader and with further increase in the impact parameter, distribution splits into two Gaussians (at target and projectile rapidities), which indicates that IMFs are coming from both participant as well as spectator matter. As the impact parameter increases, more and more energy is needed to break the colliding pair into a large number of IMFs. At peripheral geometries, the formation of heavy fragments dominates and very few number of IMFs are emitted and that IMFs are coming from spectator zone and already cooled down. We also see from fig. that due to violent nature of the reaction at higher incident energy, lighter fragments will come

from participant zone and the contribution of participant (spectator) matter towards IMFs decreases (increases).

As a next step, we extend the same studies for isobaric pairs having composite system mass equal to 68 units. In Fig. 4, we display the impact parameter dependence of $\langle N_{IMF}\rangle^{max}$ (upper panel) and $E_{c.m.}^{max}$ (lower panel) for isobaric pairs. From Fig. 4(a), we find that $\langle N_{IMF}\rangle^{max}$ shows a "rise and fall" with an increase in the impact parameter except for the reaction of

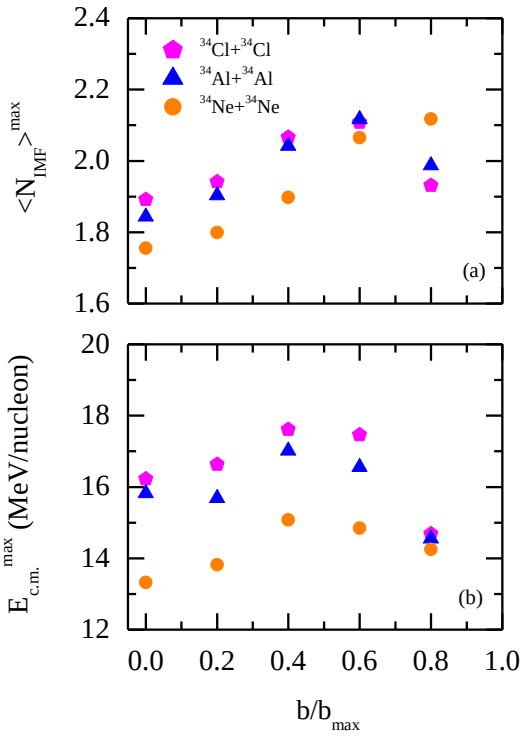

Fig. 4. (Color Online) Same as Fig. 2 but for isobaric pairs.

^{34}Ne+^{34}Ne. This may be due to large neutron content (N/Z = 2.4) in the reaction of ^{34}Ne+^{34}Ne. At peripheral geometries, the formation of heavy fragments dominates, as a result multiplicity of IMFs should decrease. On the other hand, symmetry energy, being repulsive for neutrons, will make neutron-rich systems to boil off faster compared to neutron-poor systems and will make the neutrons to escape from the interaction zone in the primary phase of the reaction. Thereby, the multiplicity of fragments formed will fall in the range of IMFs. Also $E_{c.m.}^{max}$ shows the same behavior with increase in the impact parameter as already explained in the case of isotopic pairs. In our earlier communication [17], we studied the isospin effects on $E_{c.m.}^{max}$ and $\langle N_{IMF}\rangle^{max}$. We found that when we replace some protons into neutrons, $E_{c.m.}^{max}$ decreases. From Fig. 4(b), we find that this behavior of $E_{c.m.}^{max}$ remains preserved throughout the range of impact parameter except for b/b_{max} = 0.8. Due to the extreme low density owing to a small overlap in lighter colliding nuclei (A_{tot} = 34), IQMD model may not yield proper results for peripheral collisions. It is known that molecular dynamics models do not yield proper physics for very low density situations. This situation is further deteriorated when extreme neutron-rich nuclei are considered. As neutron content increases, the proton content will decrease which will lead to lesser number of collisions.

IV. SUMMARY

In summary, we studied the role of colliding geometry on the peak multiplicity of intermediate mass fragments, $\langle N_{IMF}\rangle^{max}$ and peak center-of-mass energy, $E_{c.m.}^{max}$ for symmetric neutron-rich colliding pairs. We found that with increase in the impact parameter, both $\langle N_{IMF}\rangle^{max}$ and $E_{c.m.}^{max}$ first increase, attains a maxima and then decreases. We also checked the role of neutron content on $E_{c.m.}^{max}$ and $\langle N_{IMF}\rangle^{max}$ by taking isotopic and isobaric colliding pairs. We found that when we replace protons into neutrons (by keeping the total system mass fixed), $E_{c.m.}^{max}$ decreases whereas $\langle N_{IMF}\rangle^{max}$ remains unaltered. This behavior of $E_{c.m.}^{max}$ is found to remain preserved throughout the range of impact parameter. We have also studied the rapidity distribution of the intermediate mass fragments at their respective $E_{c.m.}^{max}$ and also at energies below and above $E_{c.m.}^{max}$ to shed light on the contribution of participant/ spectator matter towards IMFs. Since $E_{c.m.}^{max}$ represents the energy required to make the system boil off and it can also be associated with the energy at which liquid to gas phase transition occurs. Thus, present study gives the idea how the energy required for liquid-gas phase transition varies as a function of collision geometry. This can also be verified experimentally.

REFERENCES

[1] S. Kumar *et al*., (1998, Dec.). Impact parameter dependence of the disappearance of flow and in-medium nucleon-nucleon cross section. *Phys. Rev. C* **58**, 3494; S. Kumar *et al*., (1998, Sep.). Different nucleon-nucleon cross sections and multifragmentation **58**, 1618; S. Kumar *et al*., (2008, Dec.). Medium mass fragment production due to momentum dependent interactions **78**, 064602; S. Kumar *et al*., (2010, Jan.). Effect of the symmetry energy on nuclear stopping and its relation to the production of light charged fragments. **81**, 014601; S. Goyal and R. K. Puri, (2011, April.). Formation of fragments in heavy-ion collisions using a modified clusterization method. *Phys. Rev. C* **83**, 047601.

[2] Y. K. Vermani, S. Goyal, and R. K. Puri, (2009, June). Momentum dependence of the nuclear mean field and multifragmentation in heavy-ion collisions. *Phys. Rev. C* **79**, 064611; Y. K. Vermani and R. K. Puri, (2009, April). Microscopic approach to the spectator matter fragmentation from 400 to 1000AMeV. *Euro. Phys. Lett.* **85**, 62001; Y. K. Vermani *et al*., (2010). Study of fragmentation using clusterization algorithm with realistic binding energies. *J. Phys. G: Nucl. Part. Phys.* **37**, 015105 (2010); J. Singh and R. K. Puri, (2002, Jan.). Mass dependence in the production of light fragments in heavy-ion collisions. *Phys. Rev. C* **65**, 024602.

[3] R. K. Puri and S. Kumar, (1998, May). Binary breakup: Onset of multifragmentation and vaporization in Ca-Ca collisions. *Phys. Rev. C* **57**, 2744.

[4] J. K. Dhawan *et al*., (2006, Nov.). From fusion to total disassembly: Global stopping in heavy-ion collisions. *Phys. Rev. C* **74**, 057901.

[5] C. A. Ogilvie *et al*., (1991, Sep.). Rise and fall of multifragment emission. *Phys. Rev. Lett.* **67**, 1214.

[6] M. B. Tsang *et al*., (1993, Sep.). Onset of nuclear vaporization in ^{197}Au+^{197}Au collisions. *Phys. Rev. Lett.* **71**, 1502.

[7] J. Łukasik *et al*., (2003, May). Fragmentation in peripheral heavy-ion collisions: from neck emission to spectator decays. *Phys. Lett. B* **566**, 76.

[8] S. Gautam *et al*., (2010, June). Isospin effects on the energy of vanishing flow in heavy-ion collisions. *J. Phys. G: Nucl. Part. Phys.* **37**, 085102; S. Gautam *et al*., (2011, Jan.). Isospin effects in the disappearance of flow as a function of colliding geometry. *Phys. Rev. C* **83**, 014603; R. Chugh and R. K. Puri, (2010, July). Importance of momentum dependent interactions at the energy of vanishing flow. *Phys. Rev. C* **82**, 014603.

[9] A. Jain, S. Kumar and R. K. Puri, (2011, Nov.). Influence of charge asymmetry and isospin-dependent cross section on nuclear stopping

Phys. Rev. C **84**, 057602; K. S. Vinayak and S. Kumar, (2012, July). Effect of density-dependent symmetry energy on nuclear stopping. *J. Phys. G: Nucl. Part. Phys.* **39**, 095105.

[10] D. Sisan *et al*., (2001, Jan.). Intermediate mass fragment emission in heavy-ion collisions: Energy and system mass dependence. *Phys. Rev. C* **63**, 027602.

[11] Y. K. Vermani and R. K. Puri, (2009, Aug.). Mass dependence of the onset of multifragmentation in low energy heavy-ion collisions. *J. Phys. G: Nucl. Part. Phys.* **36**, 105103; S. Kaur and Aman D. Sood, (2010, Nov.). Model ingredients and peak mass production in heavy-ion collisions. *Phys. Rev. C* **82**, 054611.

[12] Y. Yano, (2007, April). The RIKEN RI Beam Factory Project: A status report. Nucl. Instrum. Methods Phys. Res. B **261**, 1009.

[13] G. G. Adamian *et al*., (2008, Aug.). Possibility of production of neutron-rich isotopes in transfer-type reactions at intermediate energies. *Phys. Rev. C* **78**, 024613.

[14] O. B. Tarasov *et al*., (2009, Sep.). Production of very neutron-rich nuclei with a ^{76}Ge beam. *Phys. Rev. C* **80**, 034609.

[15] R. Ogul *et al*., (2011, Feb.). Isospin-dependent multifragmentation of relativistic projectiles. *Phys. Rev. C* **83**, 024608; W. Trautmann *et al*., (2008, Oct.). N/Z dependence of projectile fragmentation. *Int. J. Mod. Phys. E* **17**, 1838); C. Sfienti *et al*., (2009, April). Isotopic dependence of the nuclear caloric curve. *Phys. Rev. Lett.* **102**, 152701.

[16] V. Baran *et al*., (2002, June). Isospin effects in nuclear fragmentation. *Nucl. Phys. A* **703**, 603; F. Gagnon- Moisan *et al*., (2012, Oct.). New isospin effects in central heavy-ion collisions at Fermi energies. *Phys. Rev.C* **86**, 044617.

[17] S. Kaur and R. K. Puri, (2013, Jan.). Isospin effects on the energy of peak mass production. *Phys. Rev. C* **87**, 014620.

[18] C. Hartnack *et al*., (1998, Feb). Modelling the many-body dynamics of heavy ion collisions: Present status and future perspective. *Eur. Phys. J. A* **1**, 151; R. Bansal, S. Gautam and R. K.Puri, (2014, Feb.). J. Phys. G: Nucl. Part. Phys. **41**, 035103; S. Kumar *et al*., (2010, Jan.). Elliptical flow and isospin effects in heavy-ion collisions at intermediate energies. Phys. Rev. C **81**, 014611; S. Gautam, Raj Kumari, and R. K. Puri, (2012, Sep.). Sensitivity of transverse flow toward isospin-dependent cross sections and symmetry energy. *Phys. Rev. C* **86**, 034607.

[19] J. Aichelin, (1991, April). "Quantum" molecular dynamics—a dynamical microscopic n-body approach to investigate fragment formation and the nuclear equation of state in heavy ion collisions. *Phys. Rep.* **202**, 233.

[20] C. Sturm *et al*., (2001, Jan.). Evidence for a soft nuclear equation-of-state from kaon production in heavy-ion collisions. *Phys. Rev. Lett.* **86**, 39; C. Fuchs *et al*., (2001, Mar.). Probing the nuclear equation of state by K^+ production in heavy-ion collisions. *Phys. Rev. Lett.* **86**, 1974.

[21] R. Bansal *et al*., (2013, June). Role of structural effects on the collective transverse flow and the energy of vanishing flow in nuclear collisions. *Phys. Rev. C* **87**, 061602(R).